NASA Technical Memorandum 107257
AIAA–96–2762

Flow Coupling Effects in Jet-In-Crossflow Flowfields

D.B. Bain and C.E. Smith
CFD Research Corporation
Huntsville, Alabama

D.S. Liscinsky
United Technologies Center
East Hartford, Connecticut

J.D. Holdeman
Lewis Research Center
Cleveland, Ohio

National Aeronautics and
Space Administration

FLOW COUPLING EFFECTS IN JET-IN-CROSSFLOW FLOWFIELDS

D.B. Bain
C.E. Smith
CFD Research Corporation
Huntsville, Alabama

D.S. Liscinsky
United Technologies Center
East Hartford, Connecticut

J.D. Holdeman
NASA Lewis Research Center
Cleveland, Ohio

Abstract

The combustor designer is typically required to design liner orifices that effectively mix air jets with crossflow effluent. CFD combustor analysis is typically used in the design process; however the jets are usually assumed to enter the combustor with a uniform velocity and turbulence profile. The jet-mainstream flow coupling is usually neglected because of the computational expense. This CFD study was performed to understand the effect of jet-mainstream flow coupling, and to assess the accuracy of jet boundary conditions that are commonly used in combustor internal calculations.

A case representative of a plenum-fed quick-mix section of a Rich Burn/Quick Mix/Lean Burn combustor (i.e. a jet-mainstream mass-flow ratio of about 3 and a jet-mainstream momentum-flux ratio of about 30) was investigated. This case showed that the jet velocity entering the combustor was very non-uniform, with a low normal velocity at the leading edge of the orifice and a high normal velocity at the trailing edge of the orifice. Three different combustor-only cases were analyzed with uniform inlet jet profile. None of the cases matched the plenum-fed calculations. To assess liner thickness effects, a thin-walled case was also analyzed. The CFD analysis showed the thin-walled jets had more penetration than the thick-walled jets.

Nomenclature

$A_{orifice}$	Geometric Area of Orifice
A_{tot}	Total Flow Area in Each Axial Plane
A_i	Flow Area of Cell i
C_{avg}	$m_j/(m_j+m_\infty) = \theta_{EB}$
C_i	Jet Mass Fraction in Cell i
c_{var}	$(1/A_{TOT})\sum_i A_i (C_i - C_{avg})^2$
DR	Density Ratio ρ_j/ρ_∞
f	Mixture Fraction
h	Enthalpy
H	Duct Height
J	Momentum-Flux Ratio $(\rho_j V_j^2)/(\rho_\infty U_\infty^2)$
k_∞	Turbulent Kinetic Energy of Mainstream
m_j	Mass-Flow of Jets
MR	Mass-Flow Ratio m_j/m_∞
m_∞	Mass-Flow of Mainstream
P	Static Pressure (N/m²)
P_{exit}	Static Pressure at Combustor Exit
P_{jet}	Static Pressure of Jet
P_{s_1}	Static Pressure Upstream of Quick-Mix Orifices
P_t	Total Pressure at Plenum Entrance
P_∞	Static Pressure of Mainstream
T	Temperature (K)
T_{exit}	Exit Temperature
T_{jet}	Temperature of Jet
T_∞	Temperature of Mainstream
U_∞	Mainstream Flow Velocity (m/s)
V_j	Jet Velocity (m/s)
x	Axial Coordinate, x=0 at leading edge of the orifice
x/H	Axial Distance-to-Duct Height Ratio
y	Vertical Coordinate

American Institute of Aeronautics and Astronautics

z   Lateral Coordinate

ε_∞ Turbulent Energy Dissipation of Mainstream

ϕ_{rb} Rich-Burn Equivalence Ratio

ϕ_{lb} Lean-Burn Equivalence Ratio

ρ_{jet} Density of Jet

ρ_∞ Density of Mainstream

Introduction

The mixing of jets with mainstream flow is very significant in many gas turbine combustor applications. In conventional combustor design, air is injected through primary and dilution orifices to mix with hot gas effluent. The design of the orifices is important in combustor performance and durability (i.e. exit temperature pattern factor, exit radial temperature profile, combustion efficiency, emissions, liner hot streaks, etc.). Dilution jet mixing has received a lot of attention as discussed by Holdeman[1]. More recently, jet mixing has drawn a lot of attention in regards to low emission combustor design, especially the Rich Burn/ Quick Mix/Lean Burn (RQL)[2] combustor design. The RQL combustor requires a large amount of bypass air (typically a jet-to-mainstream mass-flow ratio of 3) to be efficiently mixed with rich burn effluent so that NO_x emissions are kept to a minimum.[3] The optimization of this type of mixing process has received a lot of study.[4-16]

CFD analysis is typically used to help design the orifice pattern for effective mixing. To conserve computer resources, CFD analysis is usually performed on the interior of the combustor; the inlet boundary conditions for the air jets are specified by the designer. The jets are typically input with uniform velocity and turbulence levels, and the flow direction is determined by 1D annulus models. Usually, an effective orifice flow area is modeled, corresponding to the geometric area multiplied by the discharge coefficient. Other research[17-21] has shown that there is a coupling effect between the annulus airflow and combustor interior flow, and the prediction of jet penetration and mixing is strongly affected by including the annulus flow in the CFD analysis. Indeed, in the next five years as parallel computers are utilized, CFD analysis will be performed starting from the compressor exit and going all the way to the combustor exit. But, for now, only the interior of the combustor is usually analyzed, and ways of defining the jet boundary conditions are needed.

McGuirk's[20-21] work focussed on primary and dilution hole airflows that had jet-to-mainstream mass-flow ratios less than 0.5. This paper studies mass-flow ratios more commonly used in RQL combustors. Instead of annulus flow, the air jets are fed by a plenum as a first step in understanding the coupling effect between jet and mainstream. A baseline plenum case is discussed first, and the nonuniformity of the jet exiting the orifice is presented. The CFD analysis is then verified by comparing isothermal numerical predictions with experimental measurements. Next, three cases of the combustor interior are analyzed to try and identify ways to specify jet boundary conditions that capture the flow coupling effects. And last, a thin-walled liner case is compared to a thick-walled liner case to assess the differences in flow coupling.

CFD Code

The approach in this study was to perform 3-D numerical calculations on generic combustor geometries with and without the addition of plenums. The code named CFD-ACE[22] was used to perform all of the computations. The basic capabilities/methodologies in CFD-ACE include:

(1)   co-located, fully implicit and strongly conservative finite volume formulation;

(2)   solution of two-and three-dimensional Navier-Stokes equations for incompressible and compressible flows;

(3)   non-orthogonal curvilinear coordinates;

(4)   multi-block grid topology;

(5)   upwind, central (with damping), second order upwind and Osher-Chakravarthy differencing schemes;

(6)   standard[23], extended, RNG[24] and low Reynolds number[25] k-ε turbulence models;

(7)   instantaneous, one-step, two-step, and four-step heat release and emission combustion models;

(8)   spray models including trajectory, vaporization, etc.; and

(9) pressure-based solution algorithms including SIMPLE and a variant of SIMPLEC.

Details Of Numerical Calculations

The focus of this study was to analyze the flow coupling effect that can occur in jet-in-crossflow geometries. The baseline configuration, shown in Figure 1, can be described as having an annular quick-mix zone section with orifices located on both the inner and outer diameter liner. The orifices are fed by plenums. The orifice length-to-diameter ratio, L/d, was greater than one, representative of a thick-walled combustor. The inner radius of the quick-mix zone annulus measured 0.3896m and the outer radius measuring 0.4404m. The height of the quick-mix zone was 0.0508m. The axial length of the calculation extended 0.152m from the leading edge of the orifice (x/H=3.0). The walls (i.e. thickness of the orifices) were modeled as being 0.0064m thick. Each orifice was fed by a plenum that was 0.065m in length and 0.076m in height. The orifices were slots with semi-circular ends and had 2:1 length-to-width aspect ratios.

To enhance the computational efficiency of the numerical calculations, only one set of orifices (top and bottom) were modeled. The orifices were located on the inner and outer diameter in the same axial plane, and inline in the transverse direction. The transverse calculation domain extended from midplane to midplane between the jets' centerline. The included angle was 3.75 degrees. Periodic boundary conditions were assumed on the transverse boundaries.

For the combustor-only calculations only the quick-mix zone was used. The quick-mix orifices were modeled as inlets with a uniform velocity profile. The velocity magnitude was determined via three different methods (Figure 2). The first method used the velocity calculated from the plenum to mixer exit pressure drop. The second method determined the pressure drop by using the total pressure in the plenum and the average static pressure across the quick-mix zone. The third method calculated a velocity based on the mass-flow through the geometric area of the orifice. The jet velocities for the three method were calculated to be; 155 m/sec, 135 m/sec, and 92 m/sec respectively.

To assess the effects of orifice thickness, a thin-walled geometry was also analyzed. The thin-walled case was identical to the baseline case except for the orifice thickness. For the thin-walled geometry the wall thickness was reduced to be 0.000889m.

The flow conditions of the mainstream and the jets were:

Mainstream		Jets	
U_∞	= 43.5 m/s	P_{jet}	= 1.03 x 10^6 N/m^2
T_∞	= 2035 K	T_{jet}	= 777 K
P_∞	= 9.72 x 10^5 N/m^2		
k_∞	= 118.0 m^2/sec^2		
ε_∞	= 5.4 x 10^4 m^2/sec^3		

$$MR = 3.20$$
$$DR = 3.20$$
$$T_{exit} = 1755 \text{ K}$$
$$\phi_{rb} = 2.0$$
$$\phi_{lb} = 0.425$$

Grids

The computational mesh was created using CFD-GEOM[26], an interactive three-dimensional geometry modeling and mesh generation software. The baseline case consisted of approximately 86,500 cells. The grid shown in Figure 1 was created with 5 domains. Each plenum was modeled as a domain as well as each orifice. The quick-mix zone was also specified as a domain and was composed of 28,329 cells, 71 cells in the axial direction (x), 19 cells in the vertical direction (y), and 21 cells in the transverse direction (z). The plenum grid was distributed as 42x29x21 cells (x,y,z, direction). The 2:1 slots were composed of 28x11 uniformly distributed cells, with 7 cells in the vertical direction to represent the combustor wall thickness (0.0064m). The grid upstream and downstream of the slots was expanded/contracted so that each cell adjacent to the slot matched the cell size in the interior of the slot. The cells in the vertical direction were compressed in the wall regions to more accurately capture wall effects.

For the combustor-only case a single domain mesh consisting of solely the quick-mix section was used. Finally, the thin-walled case was the same as the baseline case except the thickness of the orifices was reduced.

Numerics & Models

The following conservation equations were solved: u momentum, v momentum, w momentum, mass (pressure correction), turbulent kinetic energy (k), turbulent energy dissipation (ε), and mixture fraction (f). The convective fluxes were calculated using upwind differencing, and the diffusive fluxes were calculated using central differencing. The standard k-ε turbulence model was employed and conventional wall functions were used. The walls were assumed to be adiabatic. The turbulent Schmidt and Prandtl numbers were set to be 0.5. A fast chemistry (instantaneous) model was assumed. Equilibrium products were also assumed. The inlet to the rich-burn section was assumed to be the equilibrium products of a fully-burned 1.8 equivalence ratio. The fuel used was $C_{10}H_{19}$, representative of Jet A fuel.

Convergence

All error residuals were reduced at least 6 orders of magnitude, and continuity was conserved in each axial plane to the fifth decimal. A converged solution required approximately 5-7 CPU hours on a IBM RS6000 Model 560 computer. Although the cases reported in this paper were performed using the IBM RS6000, additional cases were run using the NAS C-90 computer.

Results and Discussion

Baseline Plenum-Fed Case

Figure 3 shows the temperature contours for the baseline plenum-fed case. The temperature contours are plotted in a lateral plane through the orifice centerline. The jets show near optimum jet penetration, penetrating to approximately 1/4 duct height. There is a slight difference in penetration between the outer diameter and inner diameter jets; this difference is caused by geometric differences. The coupling effect causes a non-uniformity of the jet flowfield as it exits the orifice. By examining the velocity vectors and profile at the orifice exit (Figure 4), the jet velocity non-uniformity in the jet flowfield can be seen. Because of the large L/d of the orifice, the jet velocity is essentially normal to the crossflow. A low normal velocity at the leading edge of the orifice and a high normal velocity at the trailing edge is evident.

Similarly, the static and total pressure at the orifice discharge was also non-uniform as seen in Figure 5 and 6. There is a high total pressure core in the center of the orifice, but at the edges of the orifice there is a total pressure loss. The non-uniform static pressure is further illustrated in the axial static pressure plot presented in Figure 7. The static pressure varies from 30,000 N/m^2 above combustor exit pressure to -15,000 N/m^2 below the combustor exit pressure.

Non-Reacting Validation Case

To validate the plenum-fed baseline case, it was decided to perform a thick-orifice isothermal case for which jet mixing data existed. The case selected is described below, with the comparison between numerical predications and experimental measurements.

Geometry

For the validation case, the geometry consisted of a cylindrical mixing zone with 8 round holes uniformly spaced on the can circumference. Figure 8 shows a schematic of the test geometry. The diameter of each hole was 0.0178m (0.7 inches) and diameter of the can was 0.0792m (3.88 inches). The thickness of each round hole was 0.0792m (3.12 inches). Figure 8 shows the plenum which is approximately 0.529m (6 inches) in length. The mainstream flow enters from an inlet section 0.3048m long and 0.079m in diameter. The inlet section had a divergence angle of 2 degrees with an initial diameter of 0.079m that diverges to the mixing section diameter of 0.0986m. The orifices are located 0.0508m downstream of the bulkhead that connects the mainstream inlet feed into the quick-mix region. The experimental procedure is described in, for example, Reference 14.

The computational grid is shown in Figure 9. To enhance the computational efficiency of the numerical calculations, only one orifice was modeled (45 deg. sector) and periodic boundaries were assumed. The grid was separated into three distinct blocks. The first block represented the quick-mix zone, consisting of 78 cells in the axial direction (x), 19 cells in the vertical direction (y), and 29 cells in the transverse (z) direction. The second block was the plenum; it was composed of 11 x 14 x 11 cells (x,y,z). The third block represented the orifice, composed of 29 x 29 uniformly distributed cells. The orifice was modeled with 14 cells in the

vertical direction to represent the thickness of the combustor wall. In the quick-mix section, the grid upstream and downstream of the orifice region was expanded/contracted so that each cell adjacent to the orifice region matched the cell size in the slot region. The cells in the vertical direction were compressed in the vicinity of the wall to more accurately capture wall effects.

Flow Conditions

The flow conditions of the mainstream and jets were specified to be:

Mainstream		Jets	
U_∞	= 4.637 m/s	P_{jet}	= 106,166 N/m²
T_∞	= 291.67 K	T_{jet}	= 291.67 K
P_∞	= 101,341 N/m²		
k_∞	= 2.9027 x 10⁻² m²/sec²		
ε_∞	= 3.2063 x 10⁻¹ m²/sec³		

The mass-flow ratio was specified to be 1.0 corresponding to a momentum-flux ratio of 30.

Validation Case Results

Shown in Figure 10 are the jet mixture fraction axial slices measurements. The comparable numerical results are also presented in Figure 10. Axial slices were extracted at x/R locations of 1.28, 1.54, and 2.05 downstream of the leading edge of the round hole. The same color bar was used for the calculated results and experimental measurements. The numerical results show very good agreement with the experimental results at all of the downstream stations. At the closest station (x/R=1.28), the computational results capture the center mainstream core along with the slight bluish contour levels present at about mid-radius. Moving to the farther downstream locations, the numerical results show a slightly slower mixing rate than seen in the experimental results.

Figure 11 shows the spatial unmixedness curves for the CFD and experimental results. Planar unmixedness,U_s,[27] is a parameter that quantifies the unmixedness of a distribution and can be defined as:

$$U_s = c_{var} / [c_{avg} (1-c_{avg})]$$

Good overall agreement can be seen. Thus, from an engineering viewpoint, the plenum-fed calculations capture the overall characteristics of the jets-in-crossflow.

Combustor-Only Calculations

Shown in Figure 12 are the results of the combustor-only calculations for three specified uniform inlet velocities: 1) jet velocity corresponding to the overall pressure drop velocity, 155 m/sec; 2) jet velocity corresponding to the average pressure drop velocity, 135 m/sec; and 3) jet velocity corresponding to the mass-flow through the orifice geometric area, 92 m/sec. Compared to the baseline calculation (Figure 3), each combustor-only case predicted jet overpenetration. The highest jet velocity produced the greatest amount of overpenetration, as evidenced by the mainstream flow being deflected to the outer wall. This is illustrated by the hotter temperatures near the ID and OD walls. The results of the lowest jet velocity (Method 3) still predicted overpenetrating jets, but gave the closest overall agreement to the baseline case results. Note that the OD near wall temperatures are hotter than the ID temperature for each case. This occurs because the office spacing is greater for the OD wall, resulting in more mainstream flow passing between the jets.

Thus it appears that there is no simple way to capture the flow coupling that occurs with plenum-fed flowfields. As discussed previously for the baseline plenum geometry, there exists non-uniformity in the jet flow at the discharge orifice plane. In order to use an inlet boundary condition for the orifice, one would have to devise a way to determine the velocity profile that correctly produces the flow non-uniformity at the orifice discharge. This includes correctly modeling the non-uniform velocity profile, turbulence quantities, and the flow angle. The determination of these factors creates potential problems because of their variation across the orifice cross-sectional area. If it was possible to ascertain an acceptable method of capturing the flow non-uniformity, there is no guarantee that this method would be generally applicable to a variety of different orifices (i.e. round holes, slanted slots, etc...,). Therefore from a design standpoint, it probably would be very difficult to accurately capture the jet coupling effect without the use of the plenums.

Effect of Wall Thickness

For completeness, analysis was performed on a thin-walled liner to asses the effect of wall thickness on the flow coupling effect. Presented in Figure 13 are the temperature contour results of the thin-walled case. Compared to the thick-walled case (Figure 3), the thin-walled geometry showed higher jet penetration and higher overall downstream mixing.

Based on the work performed by Lichtarowicz, Duggins, and Markland[28], the discharge coefficient for orifices with length/diameter ratios (L/d) between 0 and 1 vary significantly as a function of L/d. From these results, it would be safe to assume that the thin-walled configuration (L/d = 0.04) would have a smaller discharge coefficient than the thick-walled design (L/d > 1). The lower Cd in the thin-walled case would then result in an increased pressure drop across the orifice for the same mass-flow ratio. The total pressure variation for the two geometries is presented in Figure 14. The pressure drop, plenum total pressure-combustor total pressure, for the thin-walled case is about 6.5% whereas the thick-walled case has a pressure drop around 5.8%. Despite the variation in Cd, the normal velocity levels were essentially the same for both cases. The comparable normal velocity levels for both the thin and thick-walled cases are shown in Figure 15. The differences in the penetration levels for the thick and thin-walled cases can be addressed by examining the velocity profiles. The velocity flowfield for both cases exhibit similar characteristics, but one significant difference seen is that the velocity profiles for the thin-walled case are pushed farther into the mainstream flow. This inboard translation of the velocity profiles results in more jet penetration into the quick-mix zone for the thin-walled case. Thus the increased jet penetration can be directly attributed to the lower discharge coefficient and subsequently the higher pressure drop evident in the thin-walled case. The importance of modeling the flow through the orifice is thereby shown.

Conclusions

CFD analyses were performed on air jets injected into rich-burn effluent flowing in an annulus. Jet-to-mainstream mass-flow ratios (~3) typical of RQL combustors were analyzed. Two types of calculations were performed: 1) only the combustor was modeled, with the jet flow specified at the orifice discharge plane,

and 2) the jet plenum and orifice were included in the calculation domain. Results from the CFD analysis showed:

1) There exists a strong coupling between the jet flow and mainstream flow evidenced by the large velocity profile at the orifice exit.

2) This coupling effect could not be easily captured by specifying commonly-used uniform jet velocity boundary conditions for combustor-only CFD calculations.

3) The only way to accurately predict jet-in-crossflow flowfields is to include both the interior and exterior (plenums) flowfields in the CFD analysis. To do this, an order of magnitude increase in the number of computational cells is needed over conventional computational grid sizes.

4) CFD analysis was able to capture the effect of liner thickness on jet penetration and mixing, provided the calculation domain included the external and internal combustor geometry.

References

1. J. D. Holdeman, "Mixing of Multiple Jets with a Confined Subsonic Crossflow," *Progress in Energy and Combustion Sciences*, Vol. 19, pp. 31-70, 1993. (See also NASA TM 104412, 1991 and AIAA 91-2458, 1991.)
2. R. J. Shaw, "Engine Technology Challenges for a 21st Century High Speed Civil Transport," *AIAA Tenth International Symposium on Air Breathing Engines*, September 1-6, 1991 (Also NASA TM 104363).

3. S. A. Mosier and R. M. Pierce, "Advanced Combustion Systems for Stationary Gas Turbine Engines," Vol. 1, EPA Contract 68-02-2136, 1980.

4. J. D. Holdeman, D. S. Liscinsky, V. L. Oechsle, G. S. Samuelsen, and C. E. Smith, "Mixing of Multiple Jets with a Confined Subsonic Crossflow in a Cylindrical Duct," Accepted for publication in *Journal of Engineering for Gas Turbines and Power*, 1996 (Also ASME Paper-GT-482 & NASA TM 107185).

5. C. E. Smith, M. V. Talpallikar, and J. D. Holdeman, "A CFD Study of Jet Mixing in Reduced Flow Areas for Lower Combustor Emissions," AIAA 91-2460, June 1991 (Also NASA TM 104411).

6. D. B. Bain, C. E. Smith, and J. D. Holdeman, "CFD Mixing Analysis of Jets Injected from Straight and Slanted Slots into Confined Crossflow in Rectangular Ducts," AIAA 92-3087, June 1992 (Also NASA TM 105699).

7. D. S. Liscinsky, B. True, A. Vranos, and J. D. Holdeman, "Experimental Study of Cross-Stream Mixing in a Rectangular Duct," AIAA 92-3090, June 1992 (Also NASA TM 106194).

8. D. S. Liscinsky, A. Vranos, and R. P. Lohmann, "Experimental Study of Crossflow Mixing in Cylindrical and Rectangular Ducts," NASA CR 187141, March 1993.

9. D. S. Liscinsky, B. True, and J. D. Holdeman, "An Experimental Study of Crossflow Jet Mixing in Rectangular Ducts," AIAA-93-2037, June 1993 (Also TM 106152).

10. D. B. Bain, C. E. Smith, and J. D. Holdeman, "CFD Mixing Analysis of Axially Opposed Rows of Jets Injected in Confined Crossflow," *Journal of Propulsion and Power*, Vol. 11, No. 5, p. 885-893, September-October 1995 (See also AIAA Paper 93-2044 and NASA TM 106179).

11. D. B. Bain, C. E. Smith, and J. D. Holdeman, "CFD Assessment of Orifice Aspect Ratio and Mass Flow Ratio on Jet Mixing in Rectangular Ducts," AIAA Paper 94-0218, January 1994 (Also NASA TM 106477).

12. D. S. Liscinsky, B. True, and J. D. Holdeman, "Mixing Characteristics of Directly Opposed Rows of Jets Injected Normal to a Crossflow in a Rectangular Ducts," AIAA Paper 94-0217, January 1994 (Also NASA TM 106477).

13. D.S. Liscinsky, B. True, and J.D. Holdeman, "Crossflow Mixing of Noncircular Jets," *Journal of Propulsion and Power*, Vol. 12, No. 2, pp. 225-230, January-February 1996 (See also AIAA Paper 95-0732 and NASA TM 106865).

14. Th. Doerr and D. K. Hennecke, "The Mixing Process in the Quenching Zone of the Rich-Lean Combustion Concept," *AGARD 81st Symposium on Fuels and Combustion Technology for Advanced Aircraft Engines*, Colleferro, NR Rome, Italy, May 10-14, 1993.

15. Th. Doerr, M. Blomeyer, and D. K. Henneke, "Optimization of Multiple Jets Mixing with a Confined Crossflow," ASME Paper 95-GT-313, 1995.

16. Th. Doerr, M. Blomeyer, and D. K. Henneke, "Experimental Investigation of Optimum Jet Mixing Configurations for RQL-Combustors," 12th ISABE, Melborne, Aus., 1995.

17. J. F. Carrotte, and S. J. Stevens, "The Influence of Dilution Hole Geometry on Jet Mixing," *J. of Engineering for Gas Turbines and Power*, Vol. 112, No. 1, pp. 73-75, January 1990 (See also ASME Paper 89-GT-292).

18. S. J. Stevens, and J. F. Carrotte, "Experimental Studies of Combustor Aerodynamics, Part I: Mean Flowfields," *J. of Propulsion and Power*, Vol. 6, No. 3, pp. 297-304, May-June 1990 (See also AIAA Paper 87-1827, The Influence of Dilution Hole Aerodynamics on the Temperature Distribution in a Combustor Dilution Zone).

19. S. J. Stevens, and J. F. Carrotte, "Experimental Studies of Combustor Dilution Zone Aerodynamics, Part II: Jet Development," *J. of Propulsion and Power*, Vol. 6, No. 4, pp. 503-511, July-August 1990 (See also AIAA Paper 88-3274).

20. J. J. McGuirk and S. J. Baker, "Multi-Jet Annulus/ Core-Flow Mixing-Experiments and Calculations," ASME 92-GT-111, 1992.

21. J. J. McGuirk and A. Spencer, "CFD Modeling of Annulus/Port Flows," ASME 93-GT-185, 1993.

22. S. F. Owens, "CFD-ACE: Command Language Reference Manual," CFD Research Corporation, Huntsville, AL, CFDRC Report GR-92-6, 1992.

23. B. E. Launder and D. B. Spalding, "The Numerical Computation of Turbulent Flows," *Computer Methods in Applied Mechanics and Engineering*, Vol. 3, pp. 269-289, 1974.

24. Y. S. Chen and S. W. Kim, "Computation of Turbulent Flows Using an Extended k–ε Turbulence Closure Model," NASA CR-179204, 1987.

25. K. Y. Chien, "Predictions of Channel and Boundary-Layer Flows with a Low-Reynolds Number-Turbulence Model," *AIAA Journal*, Vol. 23, No. 2, 1985.

26. CFD-GEOM User Manual, Version 1.3, March 1995.

27. P. V. Danckwertz, "The Definition and Measurement of Some Characteristics of Mixtures," *Appl. Sci. Res.*, Sec. A., Vol. 3, pp. 279-296, 1952.

28. S. Lichtarowicz, R. K. Duggins, and E. Markland, "Discharge Coefficients for Incompressible Non-Cavitating Flow Through Long Orifices," *Journal Mechanical Engineering Science*, Vol. 7, No. 2, pp. 210-219, 1965.
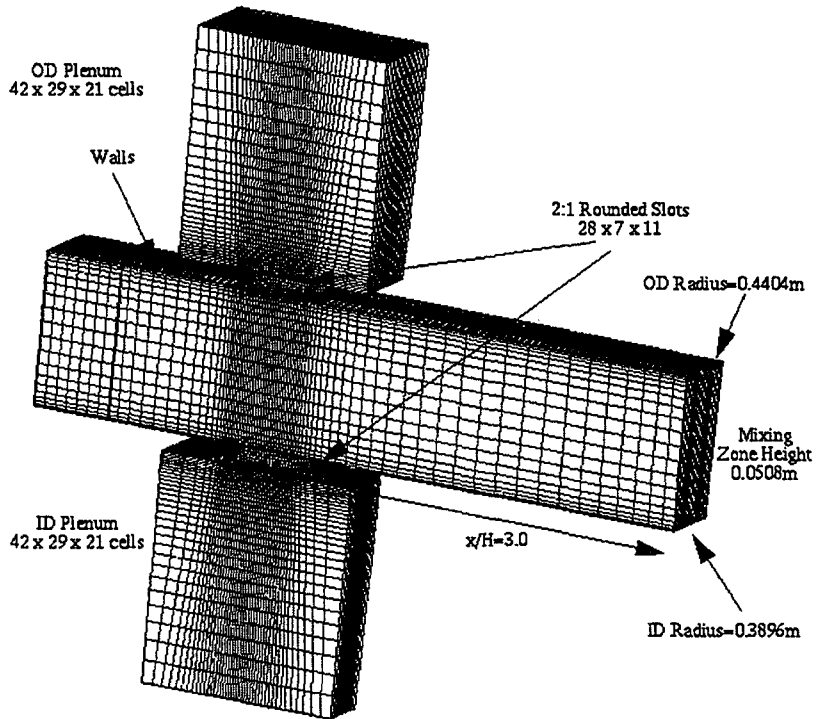
Figure 1. Baseline Annular Geometry and Grid

$$V_{jet} = \left[\frac{2\left(P_t - P_{exit}\right)}{\rho_{jet}} \right]^{1/2} \sim 155 \text{ m/s}$$

$$V_{jet} = \left[\frac{2\left(P_t - \dfrac{P_{exit} + P_{s_1}}{2}\right)}{\rho_{jet}} \right]^{1/2} \sim 135 \text{ m/s}$$

$$V_{jet} = \frac{\dot{m}_{jet}}{\rho_{jet} A_{orifice}} \sim 92 \text{ m/s}$$
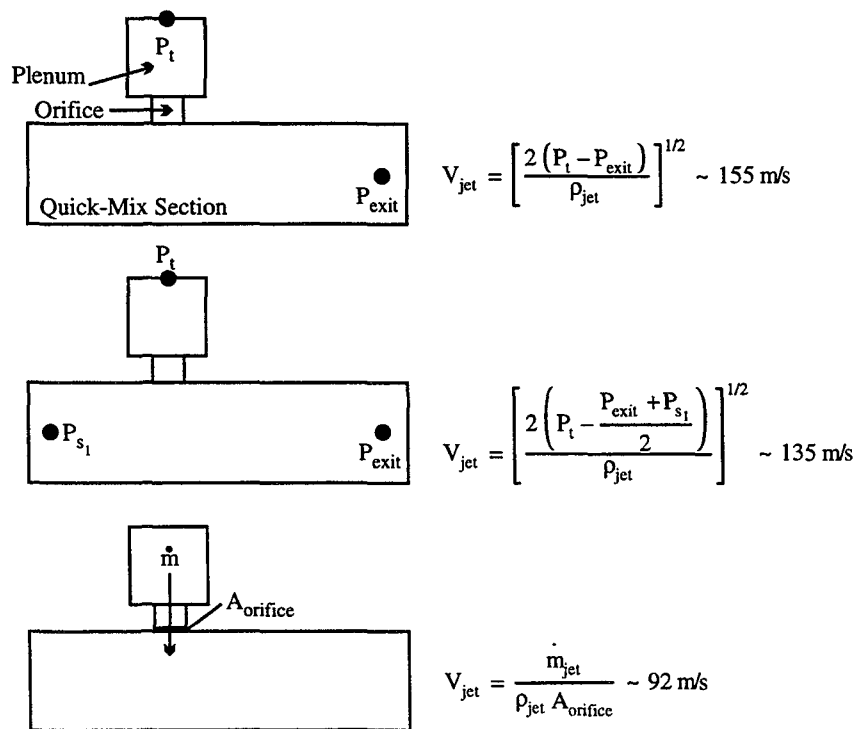
Figure 2. Three Methods Used to Determine Jet Velocity for Combustor-Only Calculations

American Institute of Aeronautics and Astronautics
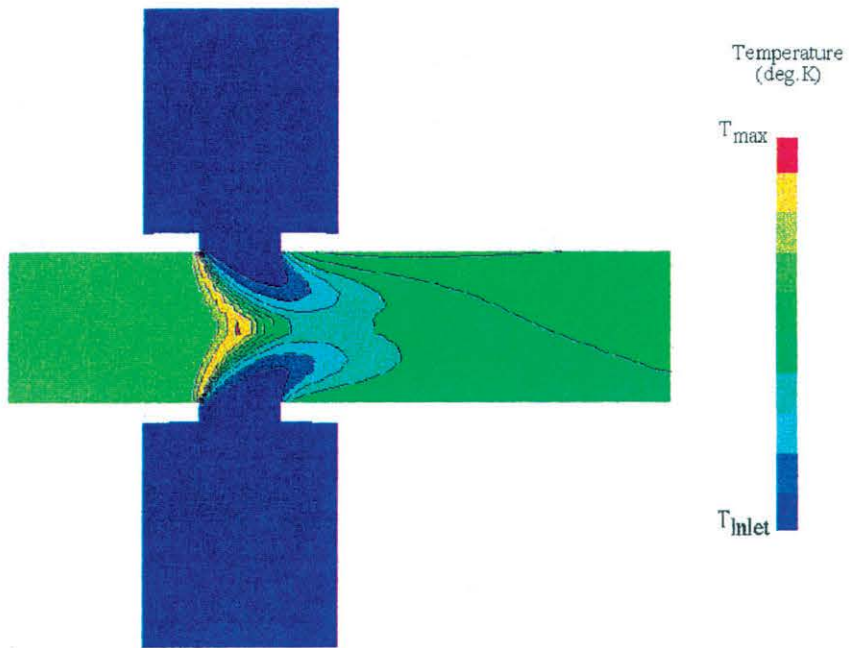
Figure 3. Temperature Contours for Baseline Plenum-Fed Geometry
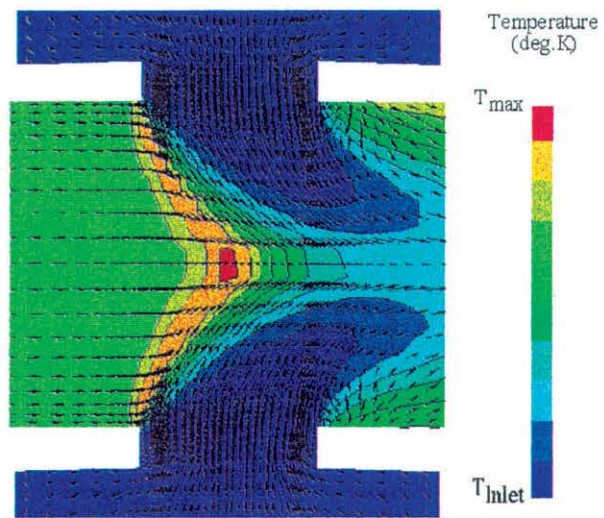
Figure 4. Close-Up of Velocity Flowfield through Thick-Walled Combustor
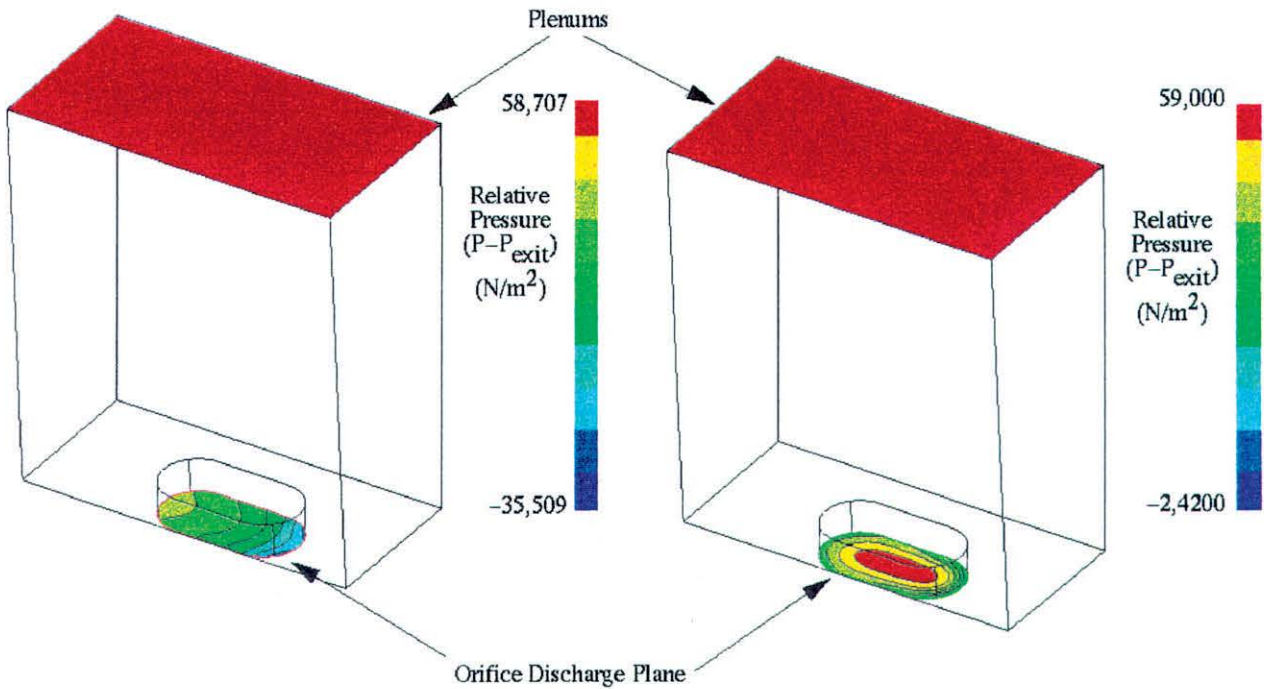
Figure 5. Non-Uniform Static Pressure Distribution Across the Orifice Exit Plane

Figure 6. Non-Uniform Total Pressure Distribution Across the Orifice Exit Plane
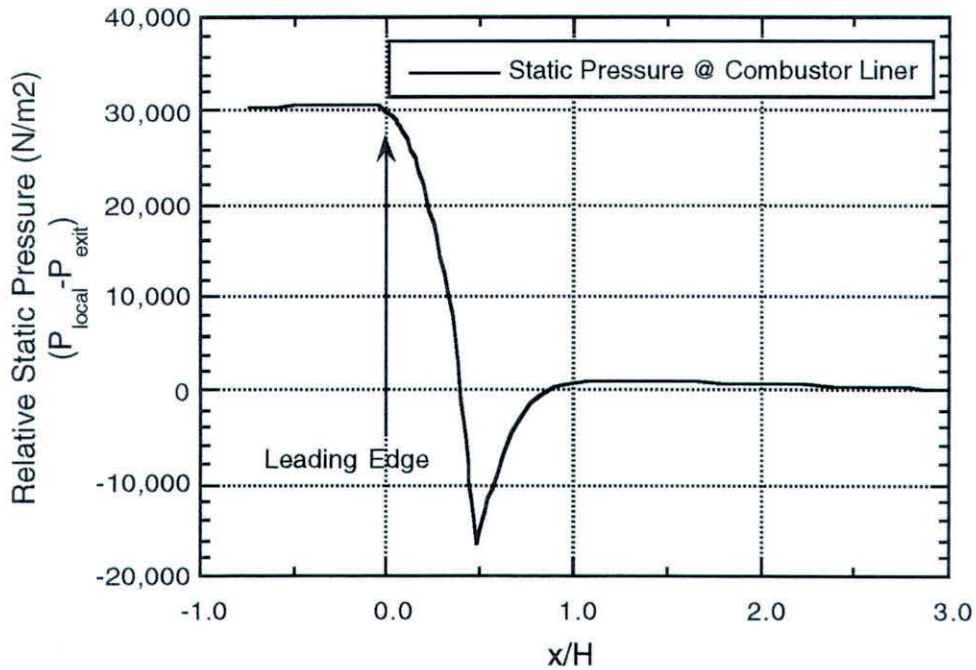
Figure 7. Non-Uniform Static Pressure at Combustor Liner (Orifice extends from 0<x/H<0.5)

View AA

2.438"

5.500"

3.875"

.7

3.88

7

10

1'-0.000"

0.312"

1.250"

AA

3.875"

4.380"

92.0°

3.110"   3.400"
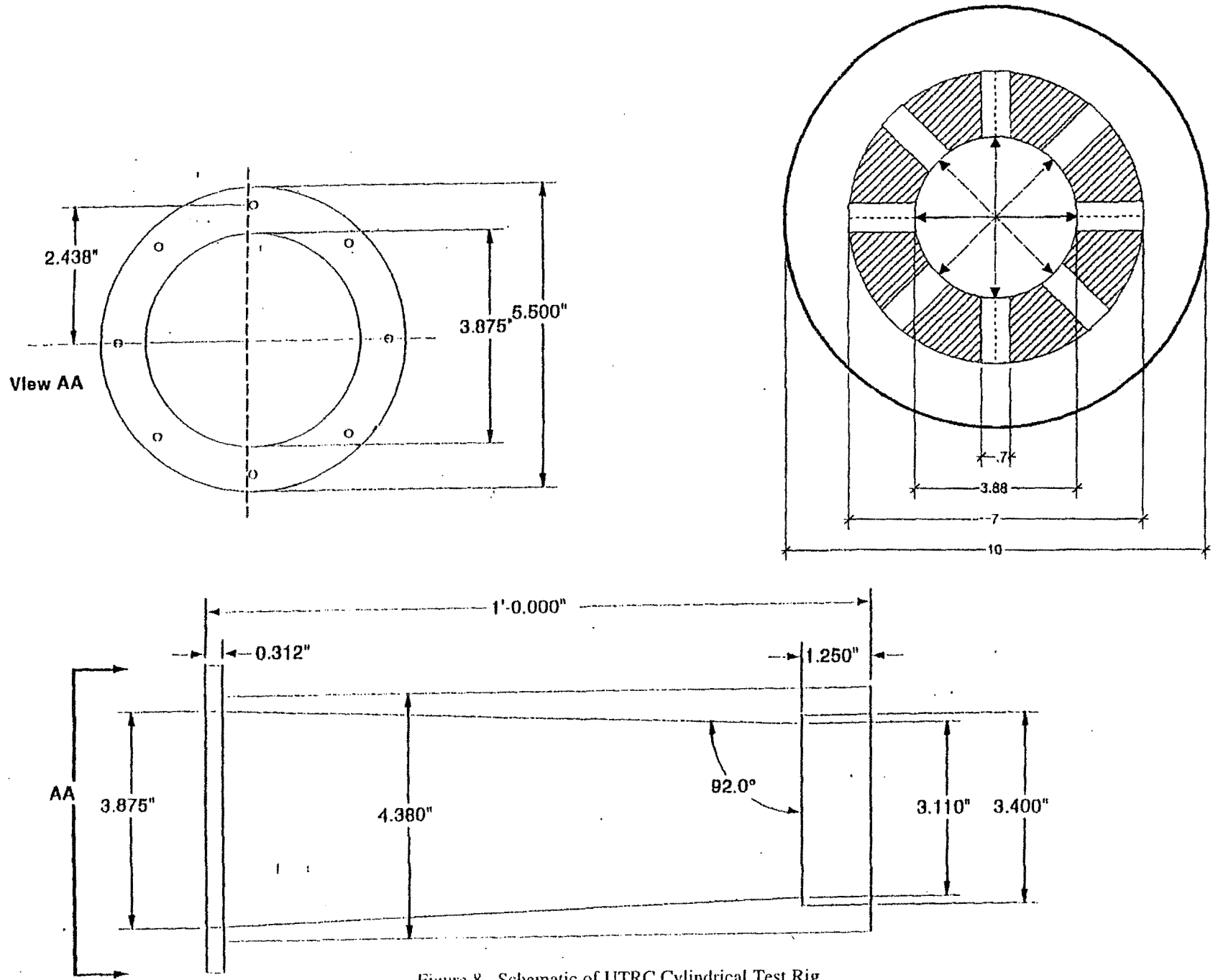
Figure 8. Schematic of UTRC Cylindrical Test Rig

Quick-Mix	78 x 19 x 29 (x,y,z)
Orifice	29 x 14 x 29
Plenum	11 x 14 x 11
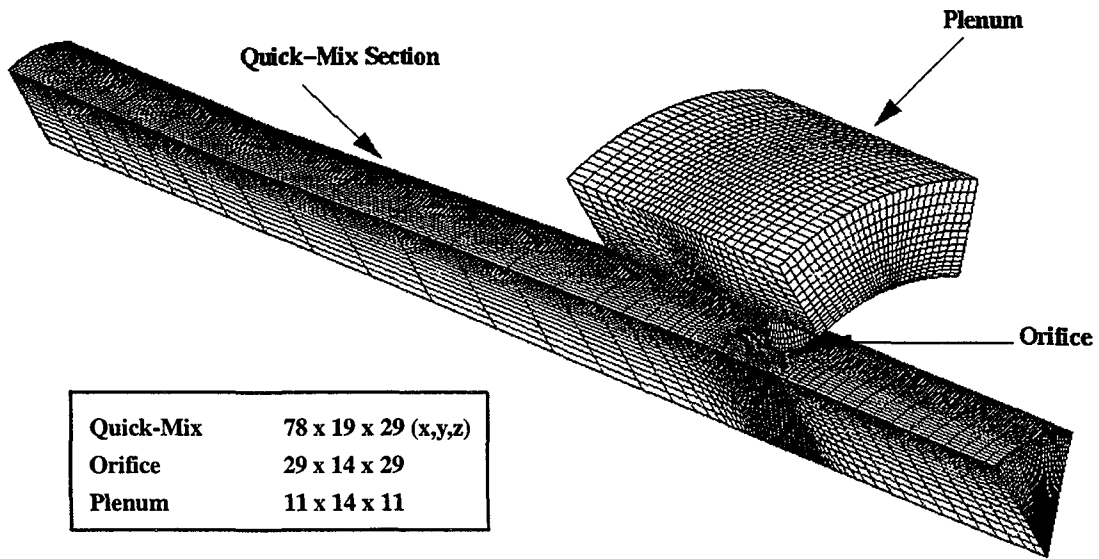
Figure 9. Computational Mesh of UTRC Cylindrical Geometry
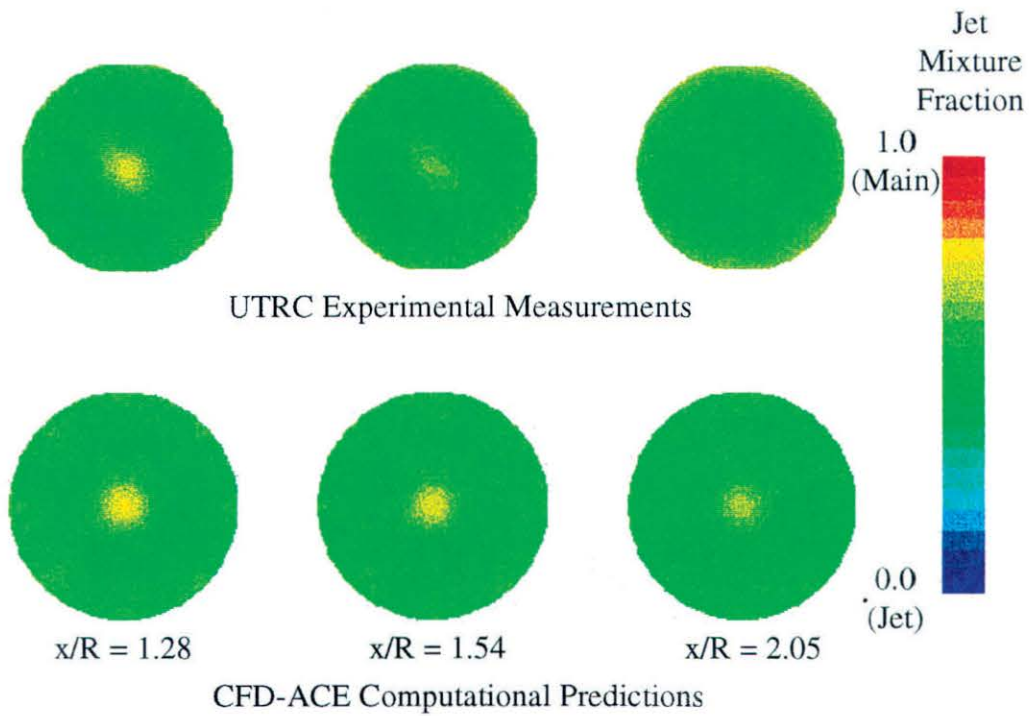
Figure 10. Comparison of CFD-ACE and Experimental Measurements
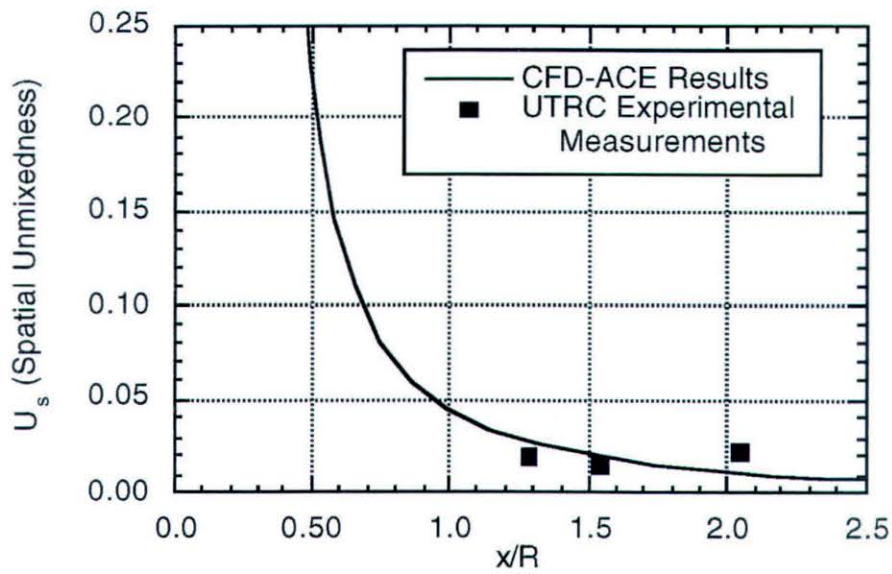
Figure 11. Numerical and Experimental Comparison of Spatial Unmixedness

Method1
(Velocity Based on Overall
Combustor Pressure Drop)

Method 2
(Velocity Based on Average Pressure Drop)

Method 3
(Velocity Based on Flow
Through Geometric Orifice Area)

T_{max}

Temperature
(deg.K)

T_{Inlet}
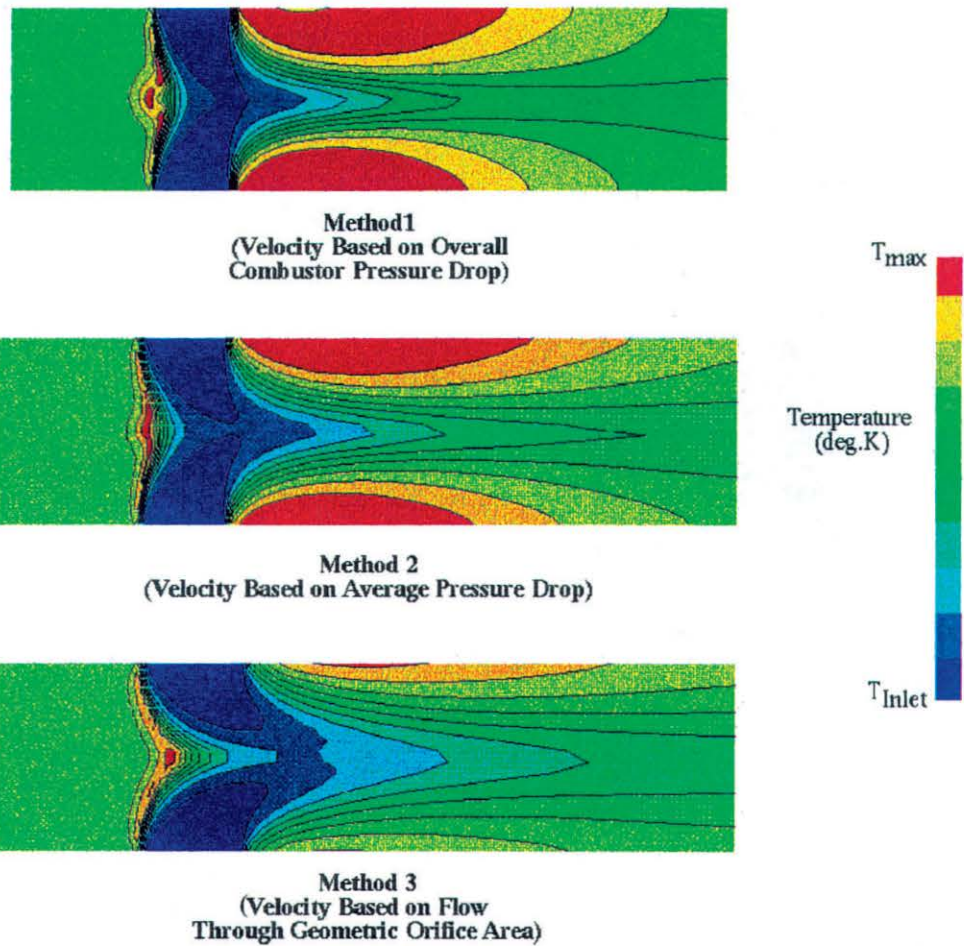
Figure 12. Combustor – Only Analysis for 4 Orifices ID & OD in 15 deg. Sector
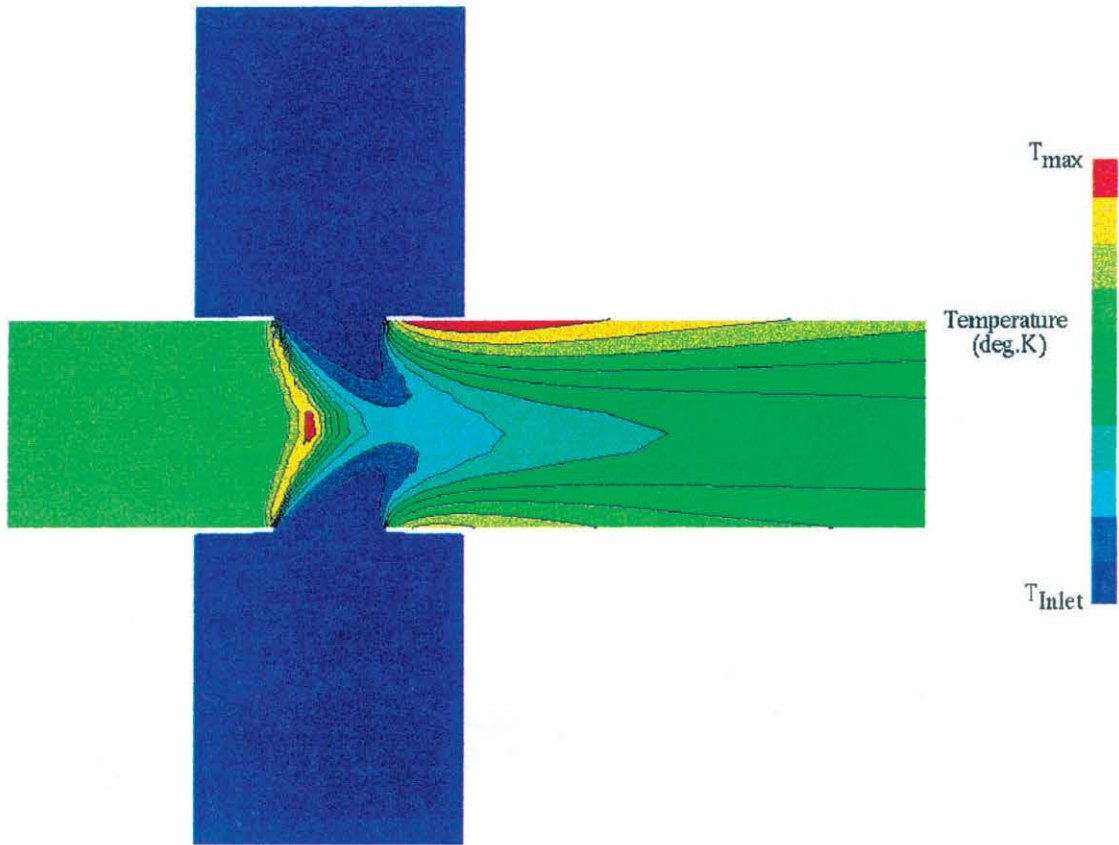
Figure 13. Temperature Contours for the Thin-Walled Geometry

Liner Thickness = 0.000889 m

Liner Thickness = 0.0064 m

Relative
Pressure
(P–P$_{exit}$)
(N/m^2)

65,000

−17,000
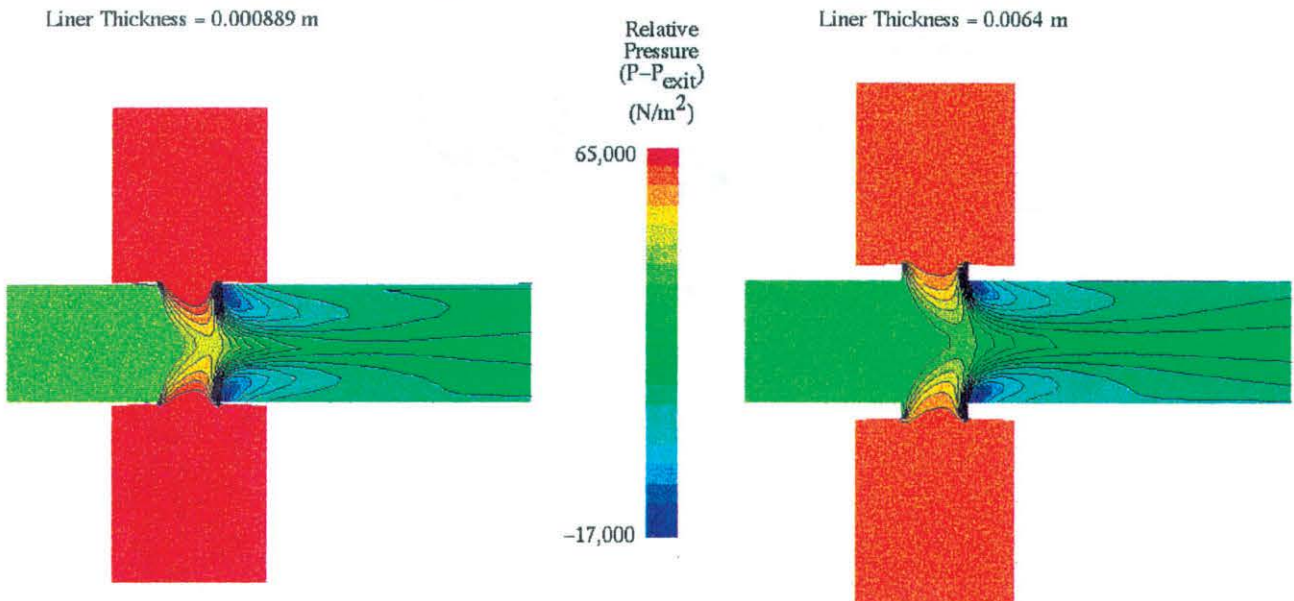
Figure 14. Total Pressure Centerline Slices for Thin and Thick-Walled Geometry

Thin−Walled Geometry

Baseline Plenum−Fed Thick−Walled Geometry

Normal Velocity
(m/sec)

155

−155
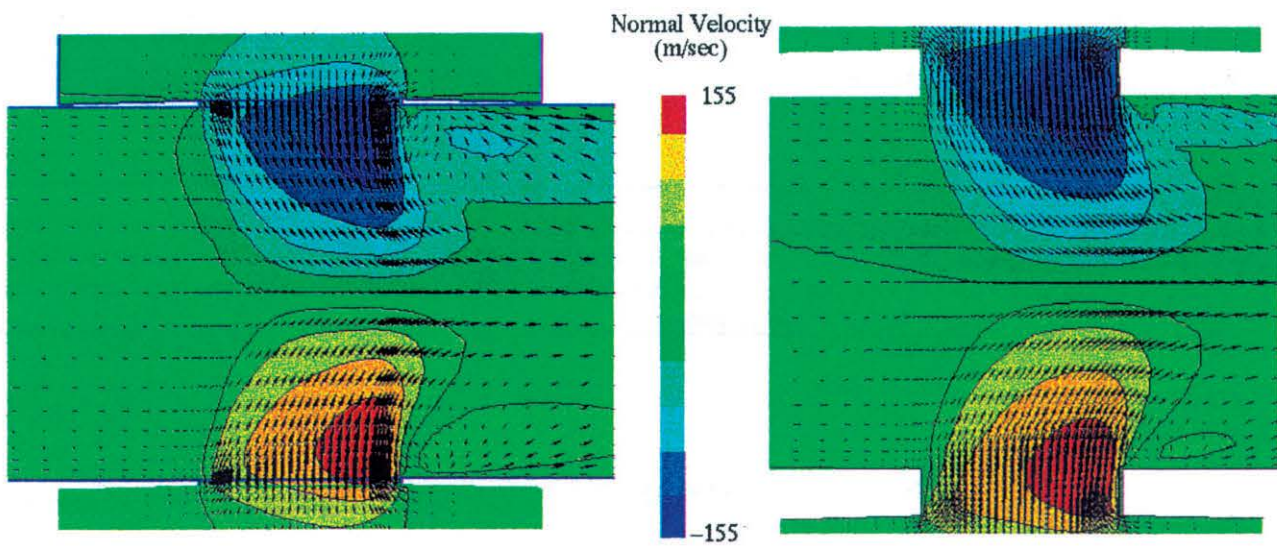
Figure 15. Velocity Profile Comparison Between Thick-Walled and Thin-Walled Combustor

REPORT DOCUMENTATION PAGE

Form Approved
OMB No. 0704-0188

1. AGENCY USE ONLY *(Leave blank)*	2. REPORT DATE June 1996	3. REPORT TYPE AND DATES COVERED Technical Memorandum

4. TITLE AND SUBTITLE

Flow Coupling Effects in Jet-In-Crossflow Flowfields

5. FUNDING NUMBERS

WU–537–02–20–00

6. AUTHOR(S)

D.B. Bain, C.E. Smith, D.S. Liscinsky, and J.D. Holdeman

7. PERFORMING ORGANIZATION NAME(S) AND ADDRESS(ES)

National Aeronautics and Space Administration
Lewis Research Center
Cleveland, Ohio 44135–3191

8. PERFORMING ORGANIZATION REPORT NUMBER

E–10318

9. SPONSORING/MONITORING AGENCY NAME(S) AND ADDRESS(ES)

National Aeronautics and Space Administration
Washington, DC 20546–0001

10. SPONSORING/MONITORING AGENCY REPORT NUMBER

NASA TM–107257
AIAA–96–2762

11. SUPPLEMENTARY NOTES

12a. DISTRIBUTION/AVAILABILITY STATEMENT

Unclassified - Unlimited
Subject Category: 07

Available electronically at http://gltrs.grc.nasa.gov/GLTRS

This publication is available from the NASA Center for AeroSpace Information, (301) 621–0390.

12b. DISTRIBUTION CODE

13. ABSTRACT *(Maximum 200 words)*

The combustor designer is typically required to design liner orifices that effectively mix air jets with crossflow effluent. CFD combustor analysis is typically used in the design process; however the jets are usually assumed to enter the combustor with a uniform velocity and turbulence profile. The jet-mainstream flow coupling is usually neglected because of the computational expense. This CFD study was performed to understand the effect of jet-mainstream flow coupling, and to assess the accuracy of jet boundary conditions that are commonly used in combustor internal calculations. A case representative of a plenum-fed quick-mix section of a Rich Burn/Quick Mix/Lean Burn combustor (i.e., a jet-mainstream mass-flow ratio of about 3 and a jet-mainstream momentum-flux ratio of about 30) was investigated. This case showed that the jet velocity entering the combustor was very non-uniform, with a low normal velocity at the leading edge of the orifice and a high normal velocity at the trailing edge of the orifice. Three different combustor-only cases were analyzed with uniform inlet jet profile. None of the cases matched the plenum-fed calculations. To assess liner thickness effects, a thin-walled case was also analyzed. The CFD analysis showed the thin-walled jets had more penetration than the thick-walled jets.

14. SUBJECT TERMS

Emissions; Dilution jet mixing; Gas turbine engine; Combustion chamber

15. NUMBER OF PAGES
19

16. PRICE CODE
A03

17. SECURITY CLASSIFICATION OF REPORT	18. SECURITY CLASSIFICATION OF THIS PAGE	19. SECURITY CLASSIFICATION OF ABSTRACT	20. LIMITATION OF ABSTRACT
Unclassified	Unclassified	Unclassified	